

Effects of Stressor Controllability on Corticostriatal Activity

George D. Trahan

Department of Psychology & Neuroscience

Dr. Michael Baratta

Thesis Advisor

Dr. Steven Maier, Department of Psychology & Neuroscience

Defense Committee Members

Dr. Jerry Rudy, Department of Psychology & Neuroscience

Dr. Dylan Taatjes, Department of Chemistry & Biochemistry

An undergraduate honors thesis submitted to the Faculty of the University of Colorado in partial fulfillment of the requirement for the degree of Honors Baccalaureate

Defended on April 7th, 2015

CONTENTS

Abstract.....	3
Introduction.....	4
Methods.....	8
Results.....	13
Discussion.....	16
Acknowledgements.....	19
References.....	20
Figure/Table Legend.....	25
Figures/Tables.....	28

Abstract

The degree of behavioral control that an organism has over a stressor potently modulates the neurochemical and behavioral consequences of that stressor. Many of the stress-induced outcomes that occur following uncontrollable stress (e.g., exaggerated fear, reduced social exploration, shuttlebox escape deficit) do not occur if the identical stressor is controllable. Furthermore, having an experience with behavioral control (time A) alters how an organism responds to future adverse events (time B), even those that are uncontrollable and occur in very different contexts (termed “behavioral immunization”). Pharmacological studies suggest that the prelimbic region (PL) of the ventral medial prefrontal cortex (vmPFC) is critical for the short- and long-term protective effects of behavioral control. The concept of behavioral control is similar to action-outcome contingency learning, which involves a circuit containing the PL and the dorsomedial striatum (DMS). Here we determine if the corticostriatal system (PL neurons that project to the DMS) is selectively activated by the presence of control (time A; Experiment 1), and whether or not prior experience with control activates this pathway during a subsequent challenge (time B; Experiment 2). Combining retrograde tract tracing with immediate-early gene immunostaining, we found that DMS-projecting PL neurons are selectively activated by behavioral control. However, this same population was not activated during exposure to a later uncontrollable stressor. Additionally, using dual fluorescent retrograde tracing, we determined that the DMS-projecting PL neurons constitute a separate population from PL neurons that exert top-down inhibitory control over limbic structures activated by adverse events (i.e., PL neurons that project to the dorsal raphe nucleus; DRN). These studies provide initial evidence that the corticostriatal circuit is recruited during the initial experience of behavioral control, but do not participate in the later resistance to challenge.

Introduction

Traumatic events have long been known to play an important role in the development and perpetuation of psychiatric disorders such as substance use disorders, depression, and anxiety disorders such as posttraumatic stress disorder (PTSD). Yet not all individuals who are subjected to traumatic events develop such disorders, and certainly not to the same extent. Although genetic factors are doubtlessly important, coping factors appear to provide resilience to such events. Behavioral control is a central aspect of coping in humans and is associated with resilience¹. In fact, behavioral control can be modeled in rats so that the underlying neurobiology of coping can be investigated. In this paradigm, subjects (rat) are placed into Plexiglas boxes with a wheel mounted in the front. The subject's tail is secured to a Plexiglas rod extending from the back of the box, and receives a series of tailshocks. One rat can terminate the tailshock by turning the wheel (escapable shock, ES), while a second rat is yoked to the first and receives the identical tailshock but has no control over its termination (inescapable shock, IS). Thus, the shock received by each rat is equivalent in both duration and intensity; the only difference between the two subjects is that one is able to terminate the tail shock of its own accord while the other cannot.

Shock is chosen as the medium for stress induction because it can be temporally controlled and can be delivered at an equivalent intensity to both subjects. It can be rapidly initiated and terminated to ensure that subjects with and without control receive an identical physical experience. In addition, the use of shock allows for the subject to readily learn an operant escape response (wheel-turn). These criteria simply cannot be met with commonly used stress paradigms such as restraint, or social isolation.

Research has shown that the degree of behavioral control an animal has over a stressful event potently modulates the behavioral and neurochemical outcomes that are induced by that event. Specifically, controllable stress (ES) drastically blunts, and even prevents, a portion² of the effects typically associated with uncontrollable stress (IS; see Table 1). Not only does behavioral control negate some of the effects of an initial stressor, it can also provide a protective effect against subsequent stressors, even when those stressors vary from the context of the first exposure³; this process is referred to as behavioral immunization. To model behavioral immunization, the above treatment is used in conjunction with a secondary stressor that is applied a week later. During this secondary stressor treatment, subjects are placed in Plexiglas tubes and are administered a series of inescapable tail shocks. Subjects that were able to exercise behavioral control during the initial stressor show reduced IS behavioral outcomes compared to subjects that were not able to exert behavioral control despite the fact that both groups were exposed to an uncontrollable stressor during the secondary treatment.

Previous research suggests that the behavioral effects of uncontrollable stress stem from the stress-induced activation and sensitization of the serotonergic (5-HT) dorsal raphe nucleus (DRN)⁴. The DRN innervates many brain regions, such as the amygdala and periaqueductal gray, that are the proximal mediators of behaviors that follow uncontrollable stress, and therefore was viewed as a likely candidate for mediating the behavioral outcomes associated with IS^{5,6,7,8,9,10,11}. It is currently understood that when an uncontrollable stressor is administered, a subpopulation of DRN 5-HT neurons become intensely activated and release 5-HT onto target structures, which subsequently leads to many of the behavioral responses seen following stress. For example, release of 5-HT onto the basolateral amygdala during IS produces an exaggerated fear response during fear conditioning¹². Similarly, release of 5-HT onto the periaqueductal gray during IS

produces reduced escape responding during shuttlebox testing. Following this intense activation, 5-HT_{1A} autoreceptors become desensitized^{13,14}. 5-HT_{1A} autoreceptors are inhibitory receptors located on the presynaptic terminals of 5-HT neurons. These autoreceptors bind excess 5-HT and inhibit further 5-HT release in order to prevent overstimulation of the postsynaptic terminal. Desensitization of these inhibitory receptors causes 5-HT neurons to become sensitized in such a manner that noxious stimuli now produce an exaggerated response compared to pre-stress conditions. The IS-induced sensitization can persist for 2-4 days if no exposure to the original stimuli occurs¹⁵; sensitization can persist for much longer periods of time if re-exposure does occur¹⁶. This mechanism has been validated by pharmacological studies that have been able to replicate, as well as eliminate, the effects of uncontrollable stress by respectively activating and deactivating^{17,18,19} 5-HT neurons within the DRN.

The effects discussed above do not occur if the stressor is controllable. How does the DRN respond differently to the stressor depending on its controllability? For a brain structure to perceive control in the tail shock and wheel-turn model, it must be able to compute that the conditional probability of shock termination given that the unfixed wheel has been turned is greater than the conditional probability of shock termination given that the unfixed wheel has not been turned. Thus, somatosensory input is required in order to sense whether the shock has terminated and whether motor functions coincided with that termination. The ventral medial prefrontal cortex (vmPFC) likely serves as a detector of behavioral control for two reasons. Firstly, the vmPFC is a cortical structure that receives somatosensory input²⁰. Secondly, the DRN receives almost all of its cortical inputs from the prelimbic region (PL) region of the vmPFC²¹. Other studies have shown that the vmPFC provides glutamatergic input to GABAergic interneurons within the DRN²². The above suggests that when a subject has a controlling

response over a stressful event, the vmPFC projections to GABAergic interneurons within the DRN become activated and subsequently inhibit 5-HT release, thereby preventing the effects of tailshock (see Figure 1). By using muscimol to inactivate the vmPFC during ES treatment, Amat et al.²³ confirmed that the vmPFC is necessary for the protective effects of ES to manifest. Animals injected with muscimol prior to ES presented 5-HT levels and behavioral outcomes that were essentially equivalent to animals that had undergone IS treatment. Other studies have also shown that vmPFC activation is necessary during subsequent stressor exposure in order to provide the protective effects seen in ES subjects^{23,24,25}. The later adverse event does not have to incorporate shock as the stressor. For example, it has been shown that a prior experience with control blunts the neurochemical and behavioral outcome of social defeat.

Recent research has implicated the role of the dorsomedial striatum (DMS) in stressor controllability. The reason for this interest in the DMS stems from the similarities between behavioral control and the act-outcome learning system. The DMS is known to be a critical component in action-outcome based learning^{26,27}. Action-outcome based learning is arguably the motivating factor for the detection of a controllable stressor. Subjects used in the behavioral control paradigm effectively learn an association between turning a wheel and shock termination, which could be interpreted as an act-outcome system. Terminating the tail shock (outcome) represents a goal that can be accomplished by turning the wheel (action). A study conducted by Amat et al.²⁸ showed that DMS Fos levels were elevated following ES treatment, whereas IS treatment did not show a significant increase in Fos. Fos refers to the protein synthesized from the c-Fos immediate early gene (IEG) and is an indicator of cellular activity due to the fact that it is reliably and rapidly transcribed following neuronal activation²⁹. The study by Amat et al. also provided evidence that pharmacological inactivation of the DMS during an acute controllable

stressor produced behavioral effects similar to that of an animal that had undergone IS treatment²⁸. This suggests that the DMS is involved in the detection of behavioral control.

Methods.

Subjects

In all experiments, rats were male Sprague-Dawley rats (Harlan Labs) weighing 254–336 g (Avg. 298 ± 20.7 g), housed two per cage on a 12-h light/12-h dark cycle (on at 0700 and off at 1900h). Rats were allowed one week, prior to surgery, to adjust to the new colony after arriving at the University of Colorado Boulder campus. Experiments were conducted between 0800 and 1900h. All procedures were approved by the Institutional Animal Care and Use Committee of the University of Colorado at Boulder.

RetroBeads

RetroBeads are produced by Lumafluor. They are described as fluorescent latex microspheres that are retrogradely transported to cell bodies within a minimum of 24 hours after injection. RetroBead fluorescence can present as either green or red depending on which version of the product is used. Red RetroBeads excite at 530 nm and fluoresce at 590 nm, whereas green RetroBeads excite at 460 nm and fluoresce at 505 nm. RetroBeads were chosen in lieu of other retrograde tracers because they tend to remain concentrated at the injection site prior to retrograde transport. Other retrograde tracers typically spread out from the injection site prior to retrograde transport, which can lead to nonspecific pathway labeling. It is important to note that only red RetroBeads were used in conjunction with Alexa Fluor 488 in order to avoid spectral overlap.

RetroBead Injections and Stereotaxic Surgery

Stereotaxic surgery was carried out on a stereotaxic alignment system (Kopf) in the surgical room of the Maier/Watkins laboratory (MUEN D107) located on the University of Colorado Boulder campus. Rats were placed under anesthesia via gaseous administration of a 5% isoflurane:oxygen mixture (reagents provided by Piramal Enterprises and Airgas respectively). The dorsal portion of the cephalic region was shaved. The surgical site was then swabbed with povidone-iodine (Vedagine, Vedco). Prior to incision, adequate anesthetization was confirmed by pinching the pedal digits. If no response occurred after digital stimulation, isoflurane administration was reduced from 5% to 3%. An incision was made just posterior to the orbital region, ending just posterior to the otic region. Bregma was subsequently located; anterior / posterior (A/P) and medial / lateral (M/L) coordinates from Table 2 were used to locate the injection site. A drill (1100 7.2 V Stylus, Dremel) was used in order to gain access to the injection site. Isoflurane administration was then reduced from 3%-1.5%. A microliter syringe (Hamilton) was used in combination with a digital stereotaxic injector and controller (UMP3 and Micro 4 respectively, World Precision Instruments) in order to deliver the RetroBead solution. 300 nL (400 nL for DRN) of a 1:4 RetroBead:saline solution (reagents provided by Lumafluor and Hospira respectively) was injected into the DMS or DRN over the course of 4 min. (see Table 2 for dorsal/ventral (D/V) coordinates); an additional 10 min. was allotted for diffusion to take place. After the injection, Vetbond (3M) was used to close the surgical site. Rats were given a 10-12 day recovery period prior to testing.

Wheel-Turn Escape/Yoked Inescapable Shock Procedure

Rats received shocks in yoked pairs (ES and IS). The treatment consisted of 100 trials with an average intertrial interval of 60 s. Shock intensity was set at 1 mA for the first 33 trials,

1.3 mA for trials 34-66, and 1.6 mA for the trials 67-100. Shock intensity was increased throughout the experiment in order to elicit a reliable response from the ES subject. Shocks began simultaneously for both rats in a pair and terminated for both whenever the ES rat met a response criterion. Initially, the shock was terminated by a quarter turn of the wheel. The response requirement was increased by one quarter turn when each of three consecutive trials was completed in less than 5 s. Subsequent latencies under 5 s increased the requirement by 50% up to a maximum of four full turns (see Figure 5A). If the requirement was not reached in less than 30 s, the shock was terminated and the requirement was reduced to a single quarter turn (see Figure 5B). During the second round of treatment, rats were placed in Plexiglas tubes and stressed using the same methodology as described above. However, no avenue for shock termination was available to the rats during this second round of stress treatment.

Tissue Preparation

Two hours after the last tail-shock, rats were transcardially perfused with 100 ml of 0.9% saline containing 0.1% heparin followed by 250 ml of 4% paraformaldehyde in 0.1 M phosphate buffer (pH 7.4). Brains were removed and postfixed in the same fixative overnight. After overnight postfixation, brains were transferred to 30% sucrose containing 0.01% sodium azide and stored at 4 °C until sectioning. Brains were rapidly frozen in -40 °C isopentane and 35- μ m sections were obtained in a -22°C cryostat. Free-floating prefrontal cortex sections were stored at 4 °C in cryoprotectant until staining. Striatal sections were also taken on gelatin submerged slides (Superfrost, Fischer Scientific) in order to verify RetroBead injection placement (see Figure 4A).

Fos Staining

Prefrontal cortex tissue was washed in 0.01 M Phosphate buffered saline (PBS) prior to being placed in a 25-well basket (3-4 slices per well). Tissue was subsequently washed three times, for 10 minutes each time, with 0.5% Triton in 0.01 M PBS (PBS-T), then PBS, and then PBS-T again. The tissue was then left overnight in 2.5% bovine albumin serum in PBS-T at 4 °C. After overnight blocking, the tissue was washed again in PBS-T and PBS as is described above. The tissue was then incubated for 24 hrs. at room temperature in a 1:2000 rabbit polyclonal c-Fos antibody (sc-52, Santa Cruz Biotechnology) solution containing 2% goat serum in PBS-T. After primary antibody incubation, the tissue was washed again in PBS-T and PBS as described above. The tissue was then incubated for two hours at room temperature under aluminum foil in a 1:250 Alex Fluor 488 goat anti-rabbit solution containing 2% goat serum in PBS-T. Following secondary antibody incubation, the tissue was washed three more times for five minutes each time in PBS. The tissue was then floated onto gelatin submerged slides (Superfrost, Fischer Scientific). Once the slides were dry, they were subjected to 1-2 drops of Vectashield hardset and coverslipped.

Fos Quantification

Pictures of stained prefrontal cortex tissue were taken on a fluorescent confocal microscope. A cell counter addon for the imaging software ImageJ was used in conjunction with the image processing package Fiji in order to quantify cells that expressed RetroBeads and/or Fos protein. Note that the presence of Fos protein is inferred from the fluorescence of the secondary antibody used for Fos staining. Only the prelimbic and infralimbic regions of the prefrontal cortex were used for quantification. RetroBead labeled cells presented as red halos. Fos labeled cells presented as solid green circles. Elevated Fos levels were differentiated from basal Fos levels by reducing the green color balance within ImageJ until only the brightest Fos

cells were present. Only cells with elevated Fos expression and proper RetroBead placement were used in statistical analysis.

Statistical Analysis

The following refers to the analysis of the prelimbic and infralimbic regions of the prefrontal cortex from a single slice of brain tissue. Total RetroBead (Rb+) and Fos (Fos+) labeled cells were recorded in Microsoft excel. Cell counts were organized by region (i.e., prelimbic and infralimbic), and cortical layer (i.e., supragranular and infragranular) Cells that expressed both RetroBeads and Fos protein simultaneously, referred to hereafter as “double-labeled cells”, were divided by the total number of Rb+ cells in order to obtain a percentage of stress activated cells that project from the prefrontal cortex to the dorsomedial striatum. A One-way ANOVA was used to determine statistical significance between all treatment groups while a protected Fisher least significant difference post hoc was used to determine statistical significance between particular treatment groups.

Experimental Design

In the current study, we investigate the possibility that DMS-projecting PL neurons are differentially activated by ES and IS treatment upon exposure to an acute stressor (Experiment 1). We also determined if prior behavioral control differentially activates DMS-projecting PL neurons during later exposure to an uncontrollable stressor (Experiment 2). Lastly, this experiment looks at whether PL-to-DMS neurons are the same neurons that project to the DRN (Experiment 3). In this model, 71 rats were unilaterally injected with RetroBead retrograde tracers into the DMS prior to testing (see Methods for details). 10-12 days after injection, 58 rats were separated into three treatment groups. Rats in each group were subjected to either escapable tail shock (ES) treatment, inescapable tail shock (IS) treatment, or home cage (HC) treatment.

The difference between ES and IS treatment, as was described above, is that in the former, rats are able to turn a freely rotating wheel that will terminate a shock, although not before the shock is initiated. It should again be noted that once the shock is terminated for the ES rat, it is simultaneously terminated for the IS rat. Home cage rats were left in their cages during the duration of the experiment. 30 rats ($n[\text{HC}] = 12$, $n[\text{ES}] = 7$, $n[\text{IS}] = 11$) were sacrificed two hours after the initial treatment. The remaining 28 rats were subjected to an additional round of tail-shock seven days after initial treatment. In this second round of treatment, all groups were subjected to IS ($n[\text{HC}/\text{IS}] = 10$, $n[\text{ES}/\text{IS}] = 8$, $n[\text{IS}/\text{IS}] = 10$). A fourth control group ($n[\text{HC}/\text{HC}] = 13$) was also present that did not participate in anything other than home cage treatment for the duration of the study. Two hours following the second round of treatment, rats were sacrificed and tissue samples were collected. Previous studies have shown that two hours provides optimal Fos expression due to neuronal activation. Tissue samples of the vmPFC were stained for Fos protein in order to indicate neuronal activation. The number of cells co-labeled for both Fos and RetroBeads were divided by the total number of RetroBead labeled cells in the vmPFC in order to obtain a percentage of cells that are activated during tail shock and project to the DMS. For Experiment 3, six rats were either unilaterally injected with red RetroBeads into the DMS ($n = 3$) or injected with green RetroBeads into the DRN ($n = 3$). 10-12 days after injection, rats were sacrificed and RetroBead quantification was carried out.

Results.

Figure 2 shows the time course of experiments 1 and 2. These times were based upon previous studies that used the same tail shock and wheel-turn paradigm. Figure 3A shows the intended injection site for experiments 1 and 2, while Figure 3B shows the intended injection

sites for experiment 3. These sites were chosen based upon previous studies that identified the DRN and DMS as structures involved in stressor controllability. Figure 4A shows a picture of RetroBeads deposited within the DMS. Images were taken of each subjects' DMS to ensure that RetroBeads had been deposited into the proper location. If a subject showed a RetroBead deposit outside of the region depicted in Figure 4A, the subject was not included in the study. Likewise, Figure 4B shows RetroBead deposits within cell bodies located in the PL and IL regions; subjects that failed to show a significant amount of RetroBead deposits in these regions after experimentation were not included in the statistical analysis. Figure 4C depicts Rb+, Fos+ and double-labeled cells viewed from a fluorescent confocal microscope during quantification. Note that overlap presents as a simple overlay of red and green as opposed to a combination of the two colors. This simple overlay of fluorescent markers allowed for fairly straightforward quantification of double-labeled cells. Figures 5A and 5B show that the rats used for data analysis were able to escape in an increasingly short amount of time and learn the association between wheel-turning and tail shock termination. Rats that were unable to learn this association or meet reasonable escape latency times were not included in the study.

Experiment 1: Initial Stressor Exposure

ANOVA analysis showed no significant difference in the total number of Rb+ cell counts in either the PL supragranular ($F_{2,27} = 1.62$, $p = 0.2162$) or infragranular ($F_{2,27} = 0.24$, $p = 0.7891$) layers (graph omitted). ANOVA analysis of PL supragranular Fos+ cell counts showed no significant difference ($F_{2,27} = 3.28$, $p = 0.0533$)(see Table 3 and Figure 6A). ANOVA analysis of PL infragranular Fos+ cell counts showed a significant difference ($F_{2,27} = 16.09$, $p < 0.0001$). Post hoc analysis of PL infragranular Fos+ cell counts showed that ES and IS groups had

enhanced levels of Fos compared to the HC group ($p < 0.0001$, $p = 0.0014$ respectively). Post hoc analysis also showed increased Fos in the ES group compared to the IS group ($p = 0.0275$)(see Table 3 and Figure 6B). ANOVA analysis showed no significant difference in the percentage of double-labeled cells within supragranular layers of the PL ($F_{2,27} = 1.20$, $p = 0.7891$)(see Figure 7A). ANOVA analysis did show a significant difference in the percentage of double-labeled cells within the infragranular layers of the PL ($F_{2,27} = 10.49$, $p = 0.0004$). Post hoc analysis revealed a decrease in the percentage of double-labeled cells in HC and IS groups compared to the ES group ($p = 0.0001$, $p = 0.0031$ respectively)(see Figure 7B).

Experiment 2: Inescapable Shock Exposure 1 Week After Initial Exposure

ANOVA analysis showed no significant difference in the total number of Rb⁺ cell counts in either the PL supragranular ($F_{2,27} = 1.57$, $p = 0.214$) or infragranular ($F_{2,27} = 2.23$, $p = 0.103$) layers (graph omitted). ANOVA analysis of PL supragranular Fos⁺ cell counts showed no significant difference ($F_{2,27} = 0.73$, $p = 0.5390$)(see Table 4 and Figure 8A). ANOVA analysis of PL infragranular Fos⁺ cell counts showed a significant difference ($F_{2,27} = 6.07$, $p = 0.002$). Post hoc analysis of PL infragranular Fos⁺ cell counts showed a significant increase in ES/IS, IS/IS, and HC/IS groups compared to the HC/HC group ($p = 0.025$, $p = 0.0004$, $p = 0.002$ respectively)(see Table 4 and Figure 8B). ANOVA analysis showed no significant difference in the percentage of double-labeled cells within the supragranular layers of the PL ($F_{2,27} = 1.40$, $p = 0.259$)(see Figure 9A). ANOVA analysis did show a significant difference in the percentage of double-labeled cells within the infragranular layers of the PL ($F_{2,27} = 3.30$, $p = 0.032$). Post hoc analysis revealed a significant increase in IS/IS and HC/IS groups compared to the HC/HC group ($p = 0.0043$, $p = 0.0486$ respectively)(see Figure 9B).

Experiment 3: DMS and DRN Double RetroBead Labeling

Figure 10A depicts cells labeled with red or green RetroBeads. Cells presenting red RetroBeads project to the DMS, while green cells project to the DRN. Cells that present both red and green RetroBeads would project to both the DMS and DRN. Figure 10B suggests that PL cells project to either the DMS or DRN exclusively. Very few cells were seen that presented both RetroBead colors.

Discussion.

The aim of this study was to examine whether stressor controllability differentially activated cells within the PL at an initial time point (acute) and/or at a later time point (immunization) where controllability was not available. We also investigated whether cell populations that projected from the PL to the DMS and populations that projected from the PL to the DRN were one in the same. To accomplish these goals, Rb+, Fos+, and percentage of double-labeled cells were tallied and analyzed.

The consistency of Rb+ counts between treatment groups suggests that RetroBead uptake and transport are not significantly affected by stress or stressor controllability. This serves to further validate the calculation used to determine the percentage of double-labeled cells.

Fos expression within the PL supragranular layers did not appear to be affected by stress or controllability. Interestingly, the PL infragranular layers did appear to be affected by both stress and controllability. A previous study by Baratta et al.,³⁰ HC animals expressed very little Fos compared to ES and IS animals. Furthermore, the authors found no significant difference between Fos expression in ES and IS animals. One explanation for this discrepancy could be the

fact that in the current study, quantification was split between supragranular and infragranular layers as opposed to quantifying the PL as a whole. Perhaps the infragranular layers of the PL are differentially activated by control while the supragranular layers are stimulated by non-stress related activities. Fos+ cell counts in the infragranular layers at the immunization time point seemed to be significantly affected by stress, but not by control. The difference between Fos+ cell counts at the acute time point and the second time point may be due to the habituation of Fos expression over time³¹. Regardless of the above, the number of Fos expressing cells does not provide an accurate picture regarding the activation of the PL-to-DMS pathway. It is already well established that the PL innervates other structures involved in stress response and therefore many of the Fos expressing cells may simply not be involved in the PL-to-DMS pathway. Hence, double-labeled cells were used to verify that activation was taking place in PL cells that project to the DMS and not elsewhere.

The percentage of double-labeled cells within the supragranular layers of the PL appeared to differ with the presence of stress, but no statistical significance was found. Analysis of the infragranular layers showed statistically significant differential activation of DMS-projecting PL cells when the stressor was controllable. This suggests that ES preferentially activates the corticostriatal pathway. This finding fits well with previous pharmacological studies by Amat et al.²⁸, which showed that the DMS is necessary in mediating the behavioral and neurochemical outcomes that precipitate from ES treatment.

Unlike the results seen at the acute time point, the percentage of double-labeled cells in the infragranular layers of the PL did not significantly differ between IS/IS and ES/IS groups during the second time point. This seems to indicate that the activation of the corticostriatal pathway only occurs when a stressor is immediately controllable. This suggests that the

corticostriatal pathway is not directly involved in mediating the protective effects generated by ES when an animal is subjected to subsequent uncontrollable stress. Rather, the corticostriatal pathway is likely responsible for perceiving control and conveying this information to neurons within the PL that project to the DRN. After this information is conveyed, the corticostriatal pathway is not needed for the effects of stress-induced immunization to occur.

Experiment 3 focused on determining whether PL-to-DMS and PL-to-DRN cell populations were one in the same. Figure 10B suggests that this is not the case and that the two circuits are not continuous, but rather contiguous. This means that detecting control does not occur simultaneously with the PL mediated inhibition of the DRN. It is most likely that DMS-projecting PL neurons are activated prior to DRN-projecting PL neurons assuming that the detection of controllability must happen prior to inhibition of DRN 5-HT release, although this has not been directly verified.

Future studies could utilize direct methods of neuronal activation and inhibition in order to provide a more robust link between control and the corticostriatal circuit. Optogenetics would be a prime candidate for such manipulation. Optogenetics relies on using particular frequencies of light to activate light-sensitive ion channels that have been introduced via viral transfection. This technique would be optimal for future studies because it can provide reliable temporal silencing or activation of neuronal firing. Optogenetic manipulation could be used to prevent DMS-projecting PL cells from firing during ES treatment or activate DMS-projecting PL cells during IS treatment. It would be expected that inhibiting DMS-projecting PL cells during ES treatment would produce behavioral effects typically associated with IS, while activating the same cells during IS treatment would produce effects similar to ES. Manipulation at a second time point, in which only IS is administered, should have no effect at all since the corticostriatal

circuit appears exhibit elevated activity only after exposure to an acute stressor. Additionally, a system using designer receptors activated by designer drugs (DREADDs) could be used to verify the findings of an optogenetic study. The DREADD system also makes use of viral-mediated gene delivery by transfecting neurons with a particular G-protein receptor that is only activated by clozapine N-oxide (CNO) or other synthetic ligands. CNO does not interact with endogenous receptors and therefore allows for very precise pharmacological manipulation of targeted cells. Unlike optogenetics, the DREADD system is not temporally precise. However, it is very clean compared to typical pharmaceutical approaches and has an advantage over optogenetics in that it more closely mimics natural neurological interactions. Using these two systems in tandem could provide causal evidence that the corticostriatal pathway is both necessary and sufficient for the behavioral and neurochemical effects of controllable stress to manifest.

Acknowledgements

I would personally like to thank Dr. Michael Baratta for his superb guidance throughout this project. Dr. Baratta taught me essentially every technique used in this paper and without his help, I would not have been able to accomplish such an endeavor. I would like to thank Dr. Steven Maier for allowing me to work in his laboratory. Working in the Maier/Watkins laboratory has been paramount to the continuation of my scientific career and has been a fantastic experience. I also want to thank Samuel Dolzani as well as Renzo Laynes for their assistance with surgical and other lab procedures. Lastly, I would like to thank Dr. Jolien Tyler for her help with fluorescent microscopy imaging.

References

- [1] Averill, J. R. (1973). Personal control over aversive stimuli and its relationship to stress. *Psychological bulletin*, 80(4), 286.
- [2] Woodmansee, W.W., Silbert, L.H., & Maier, S.F. (1993). Factors that modulate inescapable shock-induced reductions in daily activity in the rat. *Pharmacol Biochem Behav.*, 45(3), 553–559.
- [3] Maier, S.F., Amat, J., Baratta, M.V., Paul, E., Watkins, L.R. (2006). Behavioral Control, the Medial Prefrontal Cortex, and Resilience. *Dialogues in Clinical Neuroscience*, 8.4, 397–406.
- [4] Grahn, R.E., Will, M.J., Hammack, S.E., Maswood, S., McQueen, M.B., Watkins, L.R., Maier, S.F. (1999). Activation of serotonin-immunoreactive cells in the dorsal raphe nucleus in rats exposed to an uncontrollable stressor. *Brain Research*, 826, 35-43.
- [5] Gonzalez, L., Andrews, N., File, S. (1996). 5-HT_{1A} and benzodiazepine receptors in the basolateral amygdala modulate anxiety in the social interaction test, but not in the elevated plus-maze, *Brain Res.*, 732, 145–153.
- [6] Graeff, F., Brandao, M., Audi, E., Schutz, M. (1986). Modulation of the brain aversive system by gabaergic and serotonergic mechanisms. *Behav. Brain Res.*, 21, 65–72.
- [7] Iverson, S. (1984). 5-HT and anxiety. *Neuropharmacology*, 23, 1553–1560.
- [8] Lovick, T. (1994). Influence of the dorsal and median raphe nuclei on neurons in the periaqueductal gray matter: role of 5-hydroxytryptamine. *Neuroscience*, 59, 993–1000.
- [9] Ma, Q., Yin, G., Ai, M., Han, J. (1991). Serotonergic projections from the nucleus raphe dorsalis to the amygdala in the rat. *Neurosci. Lett.*, 134, 21–24.

- [10] Steinbusch, H.W.M., Nieuwenhuys, R. (1983). The raphe nuclei of the rat brainstem: a cytoarchitectonic and immunohistochemical study. *Chemical Neuroanatomy*, Raven Press, New York, 131–207.
- [11] Vertes, R. (1991). A PHA-L analysis of ascending projections of the dorsal raphe nucleus in the rat. *J. Comp. Neurol.*, 313, 643–668.
- [12] Amat, J., Matus-Amat, P., Watkins, L. R., & Maier, S. F. (1998). Escapable and inescapable stress differentially alter extracellular levels of 5-HT in the basolateral amygdala of the rat. *Brain research*, 812(1), 113-120.
- [13] Greenwood, B.N., Foley, T.E., Day, H.E. et al. (2003). Freewheel running prevents learned helplessness/behavioral depression: role of dorsal raphe serotonergic neurons. *J Neurosci.*, 23(7), 2889–2898.
- [14] Rozeske R.R., Evans A.K., Frank M.G., Watkins L.R., Lowry C.A., Maier S.F. (2011). Uncontrollable, but not controllable, stress desensitizes 5-HT_{1A} receptors in the dorsal raphe nucleus. *J. Neurosci.* 31, 14107–14115.
- [15] Maier, S.F., Coon, D.J., McDaniel, M., & Jackson, R.L. (1979). The time course of learned helplessness, inactivity, and nociceptive deficits in rats. *Learning And Motivation*, 10, 467–488.
- [16] Maier, S.F. (2001). Exposure to the stressor environment prevents the temporal dissipation of behavioral depression/learned helplessness. *Biol Psychiatry*, 49(9), 763–773.
- [17] Maier, S., Busch, C., Maswood, S., Grahn, R., Watkins, L. (1995). The dorsal raphe nucleus is a site of action mediating the behavioral effects of the benzodiazepine receptor inverse agonist DMCM. *Behav. Neurosci.*, 109, 759–766.

- [18] Maier, S., Grahn, R., Kalman, B., Sutton, L., Wiertelak, E., Watkins, L. (1993). The role of the amygdala and dorsal raphe nucleus in mediating the behavioral consequences of inescapable shock. *Behav. Neurosci.*, 107, 377–388.
- [19] Maier, S., Kalman, B., Grahn, R. (1994) Chlordiazepoxide microinjected into the region of the dorsal raphe nucleus eliminates the interference with escape responding produced by inescapable shock whether administered before inescapable shock or escape testing. *Behav. Neurosci.*, 108, 121–130.
- [20] Miller, E. K., Cohen, J. D. (2001) An integrative theory of prefrontal cortex function. *Annual Review of Neuroscience*, 24, 167–202.
- [21] Gabbott, P.L., Warner, T.A., Jays, P.R., Salway, P., and Busby, S.J. (2005). Prefrontal cortex in the rat: projections to subcortical autonomic, motor, and limbic centers. *J Comp Neurol.*, 492(2), 145–177.
- [22] Jankowski, M.P. & Sesack, S.R. (2004). Prefrontal cortical projections to the rat dorsal raphe nucleus: ultrastructural features and associations with serotonin and gamma-aminobutyric acid neurons. *J Comp Neurol.*, 468(4), 518–529.
- [23] Amat, J., Baratta, M.V., Paul, E., Bland, S.T., Watkins, L.R. & Maier S.F. (2005). Medial prefrontal cortex determines how stressor controllability affects behavior and dorsal raphe nucleus. *Nature Neuroscience*, 8.3, 365-371.
- [24] Amat, J., Paul, E., Watkins, L.R. & Maier, S.F. (2008). Activation of the ventral medial prefrontal cortex during an uncontrollable stressor reproduces both the immediate and long-term protective effects of behavioral control. *Neuroscience*, 154, 1178–1186.

- [25] Amat, J., Paul, E., Zarza, C., Watkins, L.R. & Maier, S.F. (2006). Previous experience with behavioral control over stress blocks the behavioral and dorsal raphe nucleus activating effects of later uncontrollable stress: role of the ventral medial prefrontal cortex. *The Journal of Neuroscience*, 26(51), 13264-13272.
- [26] Balleine, B.W., Dickinson, A. (1998). Goal-directed instrumental action: contingency and incentive learning and their cortical substrates. *Neuropharmacology*, 37, 407–419.
- [27] Yin, H.H., Ostlund, S.B., Knowlton, B.J., Balleine, B.W. (2005). The role of the dorsomedial striatum in instrumental conditioning. *Eur. J. Neurosci.*, 22, 513–523.
- [28] Amat, J., Christianson, J.P., Alekseyev, R.M., Kim, J., Richeson, K.R., Watkins, L.R. & Maier, S.F. (2014). Control over a stressor involves the posterior dorsal striatum and the act/outcome circuit. *European Journal of Neuroscience*, 40, 2352–2358.
- [29] Hoffman, G.E., Smith, M.S., Verbalis, J.G. (1993). c-Fos and related immediate early gene products as markers of activity in neuroendocrine systems. *Front Neuroendocrinology*, 14, 173–213.
- [30] Baratta, M.V., Zarza, C.M., Gomez, D.M., Campeau, S., Watkins, L.R. & Maier, S.F. (2009). Selective activation of dorsal raphe nucleus-projecting neurons in the ventral medial prefrontal cortex by controllable stress. *European Journal of Neuroscience*, 30.6, 1111-1116.
- [31] Struthers, W.M., DuPriest, A., Runyan, J. (2005). Habituation reduces novelty-induced FOS expression in the striatum and cingulate cortex. *Exp. Brain Res.*, 167, 136-140.

- [32] Cenci, M.A., Whishaw, I.Q., Schallert, T. (2002). Animal models of neurological deficits: how relevant is the rat? *Nat Rev Neurosci.*, 3(7), 574-579.
- [33] Nutt, D.J. (2000) The psychobiology of posttraumatic stress disorder. *Journal of Clinical Psychiatry*, 61, 24-29
- [34] Schneiderman, N., Ironson, G., & Siegel, S.D. (2005) STRESS AND HEALTH: Psychological, Behavioral, and Biological Determinants. *Annual review of clinical psychology*, 1, 607–628.
- [35] Shiflett, M.W., & Balleine, B.W. (2011). Molecular substrates of action control in cortico-striatal circuits. *Progress in Neurobiology*, 95.1, 1-13.

Figure/Table Legends

Table 1. Behavioral changes that follow exposure to uncontrollable, but not equal controllable stressor exposure.

Figure 1. Schematic of the circuits engaged by controllable (ES) and uncontrollable (IS) stress.

Abbreviations: Glu = glutamate, GABA = γ -aminobutyric acid, PAG = periaqueductal gray

Table 2. RetroBead injection coordinates for DMS and DRN. All A/P and M/L coordinates were measured from Bregma. D/V coordinates were measured from the dorsal-most portion of the brain after adjusting for A/P and M/L coordinates.

Figure 2. Schematic of experiments 1 & 2.

Figure 3. Schematic of injection sites for experiments 1-3 **(A)** Targeted RetroBead injection site for Experiments 1 & 2. Red RetroBeads were injected into the DMS of all subjects one week prior to testing. During the week preceding testing, RetroBeads were retrogradely transported to neuronal cell bodies within the vmPFC. **(B)** Targeted RetroBead injection sites for Experiments 3. Red RetroBeads were injected into the DMS of all subjects one week prior to testing. Green RetroBeads were injected into the DRN of Experiment 3 subjects one week prior to testing. During the week preceding testing, RetroBeads were retrogradely transported to neuronal cell bodies within the vmPFC.

Figure 4. Fluorescent images of RetroBead deposits as well as Rb+, Fos+, and double-labeled cells. **(A)** Post mortem fluorescent photograph of RetroBeads deposited within the DMS. Only tissue that presented similar deposits were used for cell quantification. Scale bar at bottom right represents 500 μ m. **(B)** Post mortem fluorescent photograph of RetroBeads deposited within the PL and IL of the vmPFC. **(C)** Fluorescent labeling with Fos and red RetroBeads. Fos expression is represented in green while RetroBeads are shown in red. Double-labeled cells (yellow arrow) present both RetroBeads and Fos.

Figure 5. Graphs showing wheel-turn and escape latency data. **(A)** Rats given control over stress rapidly learn to turn a wheel in order to terminate a tail shock. Initially, a quarter turn is required for the shock to be terminated. The wheel-turn requirement increased by a quarter turn upon terminating a shock in under five seconds and increased by 50% for each subsequent escape under five seconds. The wheel-turn requirement was capped at four complete rotations (16 quarter turns). **(B)** Subjects with control gradually improve their response times to terminate tail shock.

Table 3. Number of cells within the vmPFC expressing either Fos (Fos+) or RetroBead (Rb+).

Data are reported as: average(SEM), # of subjects

Figure 6. Graphs of Fos+ cell counts within the vmPFC. **(A)** Number of Fos+ cells within the supragranular (I-III) layers of the PL. **(B)** Number of Fos+ cells within the infragranular (V, VI) layers of the PL. ****P < 0.0001 compared to HC, **P < 0.01 compared to HC, # P < 0.05 compared to IS.

Figure 7. Graphs of double-labeled cell percentages within the vmPFC. **(A)** % of RetroBead-labeled cells expressing Fos within the supragranular (I-III) layers of the PL. **(B)** % of RetroBead-labeled cells expressing Fos within the infragranular (V,VI) layers of the PL. ***P < 0.001 compared to HC, ##P < 0.01 compared to IS.

Table 4. Number of cells within the vmPFC expressing either Fos or RetroBead. Data are reported as: average(SEM), # of subjects

Figure 8. Graphs of Fos+ cell counts within the vmPFC. **(A)** Number of Fos+ cells within the supragranular (I-III) layers of the PL. **(B)** Number of Fos+ cells within the infragranular (V, VI) layers of the PL. ***P < 0.001 compared to HC/HC, **P < 0.01 compared to HC/HC, *P < 0.05 compared to HC/HC.

Figure 9. Graphs of double-labeled cell percentages within the vmPFC. **(A)** % of RetroBead-labeled cells expressing Fos within the supragranular (I-III) layers of the PL. **(B)** % of RetroBead-labeled cells expressing Fos within the infragranular (V,VI) layers of the PL. **P < 0.01 compared to HC/HC, *P < 0.05 compared to HC/HC)

Figure 10. Graph of Rb+ cell counts within the vmPFC **(A)** Fluorescent labeling of the PL with red and green RetroBeads. DMS-projecting cells are represented in red while DRN-projecting cells are represented in green. **(B)** Mean number of RetroBead positive cells within the PL.

TABLE 1.

Depression-like Consequences	Anxiety-like Consequences
◆ Reduced aggression	◆ Exaggerated fear conditioning
◆ Reduced responding to aversive events	◆ Neophobia
◆ Reduced escape behavior	

FIGURE 1.

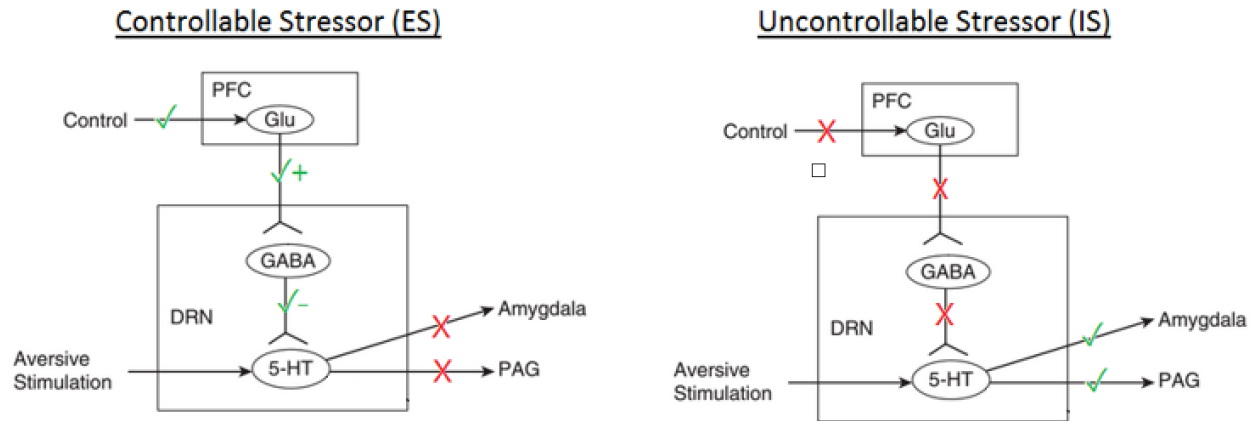


TABLE 2.

	DMS Coordinates (mm)	DRN Coordinates (mm)
Anterior / Posterior	+ 0.1	- 8.1
Medial / Lateral	\pm 2.0	\pm 0
Dorsal / Ventral	- 3.5	- 6.7

FIGURE 2.

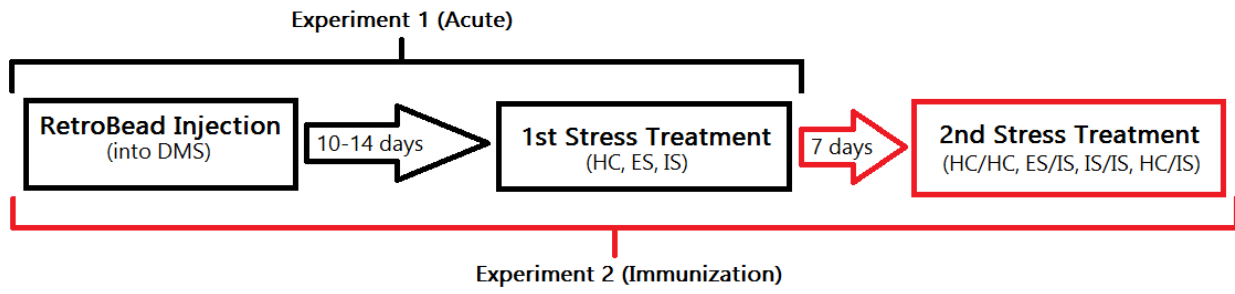


FIGURE 3.

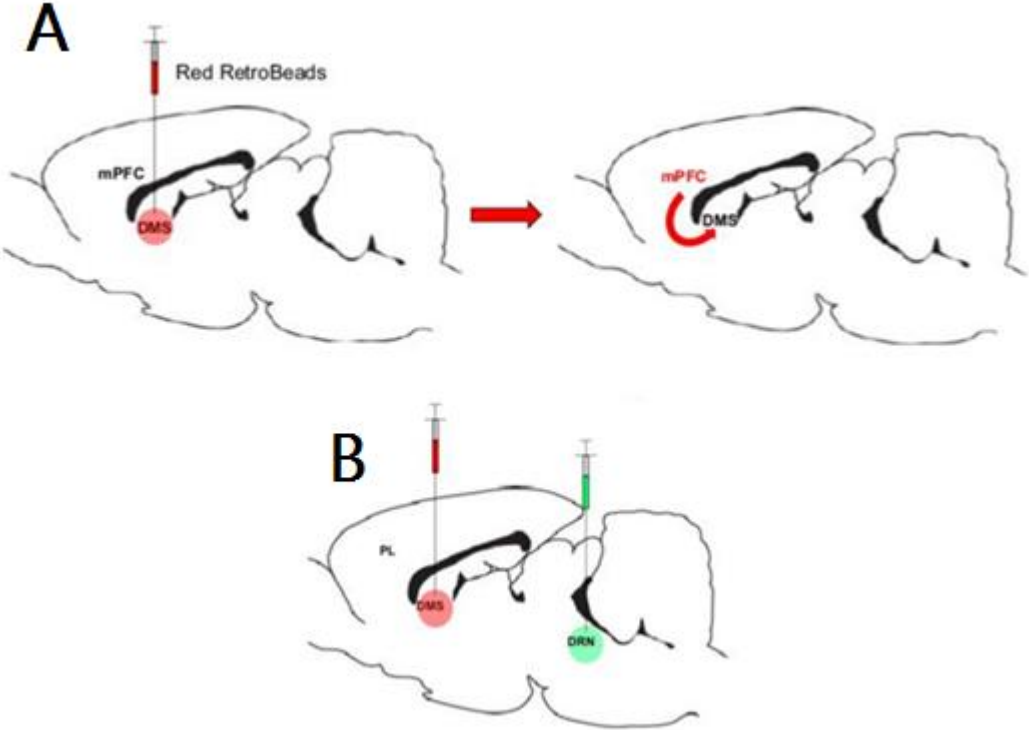


FIGURE 4.

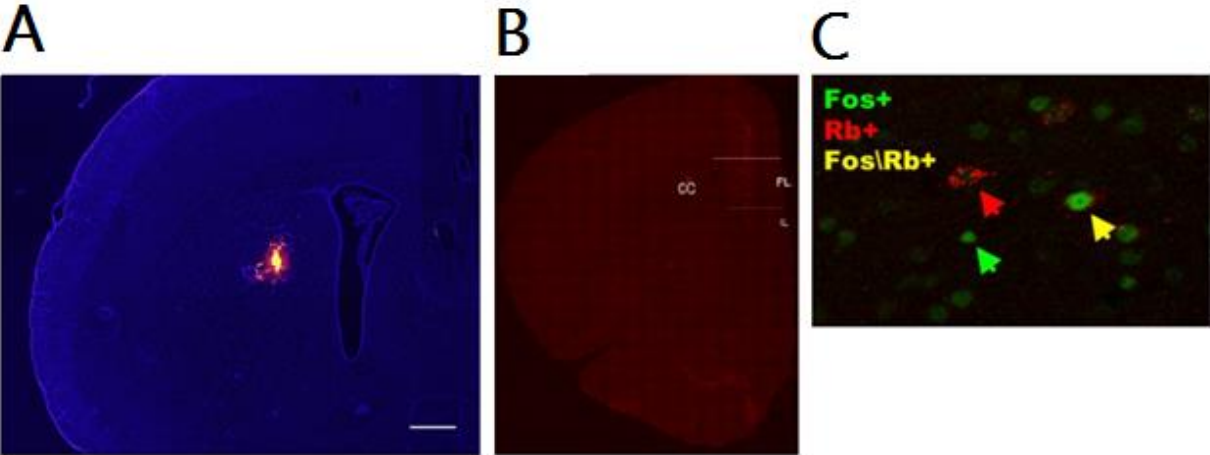


FIGURE 5.

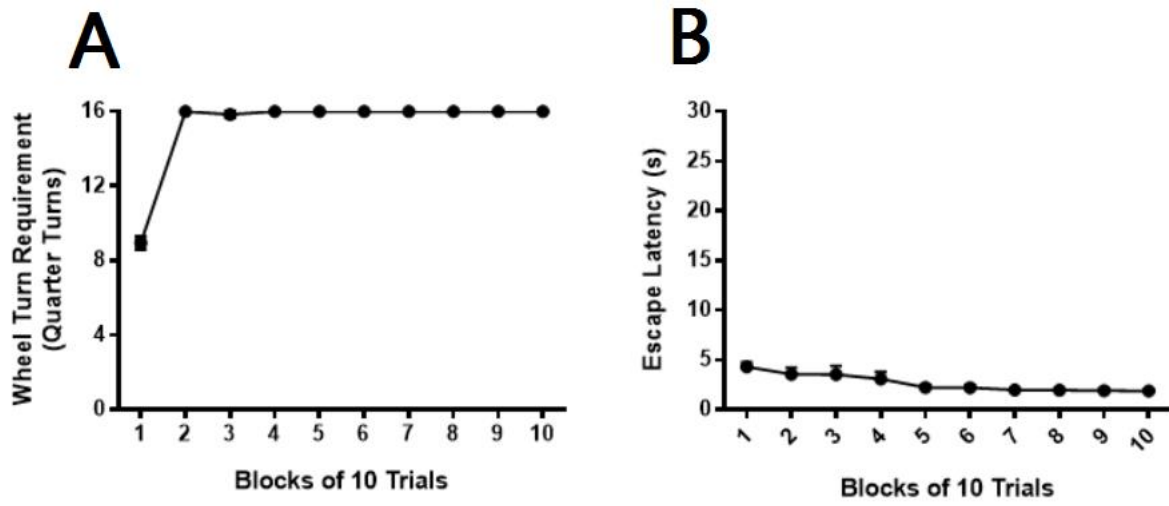


TABLE 3.

<u>Marker</u>	<u>Region</u>	<u>Layers</u>	<u>Treatment</u>		
			<u>HC</u>	<u>ES</u>	<u>IS</u>
Fos+	PL	I-III	2.83(1.09), 12	8.14(2.60), 7	5.82(0.91), 11
		V-VI	5.58(1.44), 12	27.71(4.14), 7	18.18(3.19), 11
	IL	I-III	3.00(0.84), 12	3.86(2.08), 7	1.82(0.170), 11
		V-VI	3.42(1.13), 12	15.00(1.65), 7	11.45(3.40), 11
Rb+	PL	I-III	15.58(2.31), 12	9.29(2.34), 7	13.09(2.19), 11
		V-VI	43.42(5.61), 12	44.43(5.66), 7	39.18(5.32), 11
	IL	I-III	2.17(1.13), 12	0.43(0.30), 7	1.18(0.42), 11
		V-VI	7.25(1.88), 12	5.14(2.26), 7	5.82(2.01), 11

FIGURE 6.

Acute

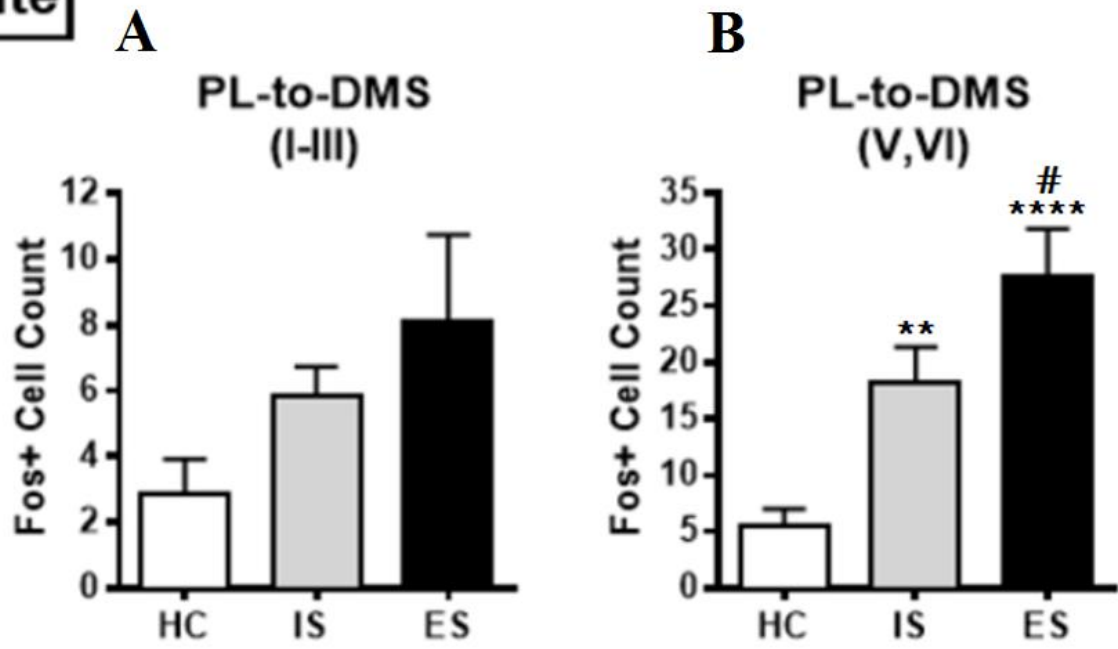


FIGURE 7

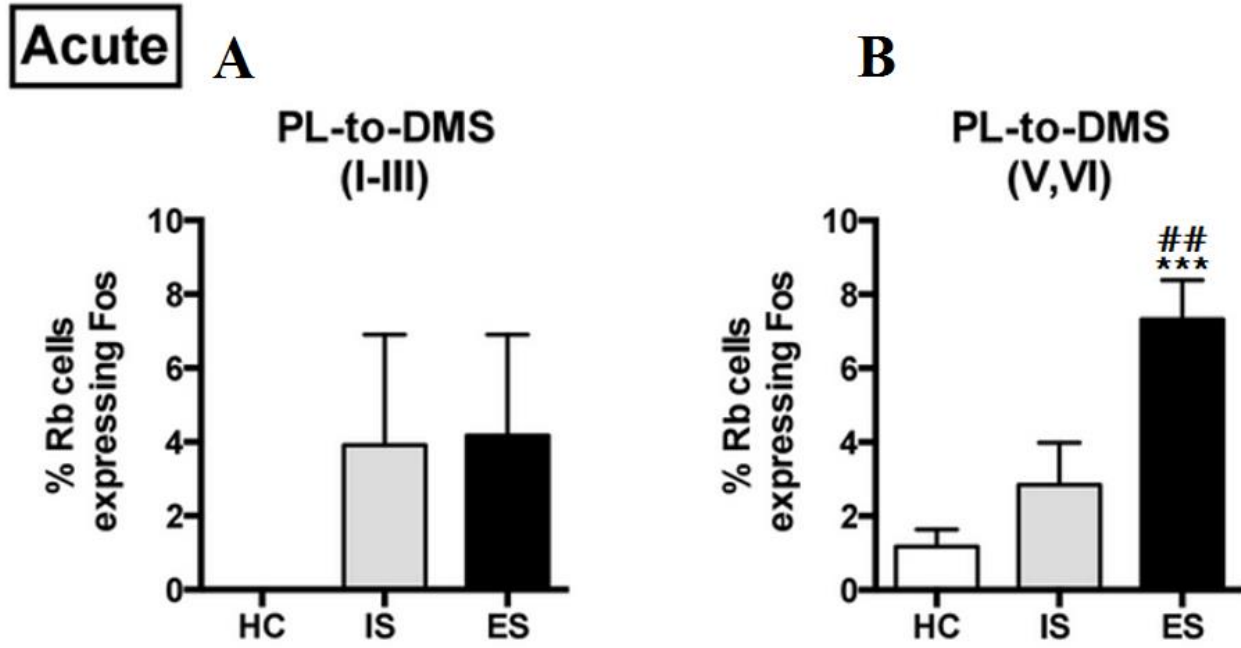


TABLE 4.

Marker	Region	Layers	Treatment			
			<i>HC/HC</i>	<i>ES/IS</i>	<i>IS/IS</i>	<i>HC/IS</i>
Fos+	PL	I-III	2.05(1.03), 10	4.56(1.55), 8	3.95(1.22), 10	3.55(1.21), 10
		V-VI	7.50(3.62), 10	19.56(3.22), 8	26.60(3.64), 10	23.75(3.36), 10
	IL	I-III	1.60(0.80), 10	2.63(0.84), 8	2.05(0.77), 10	4.00(1.40), 10
		V-VI	5.05(2.47), 10	20.00(4.22), 8	19.45(4.40), 10	22.60(4.36), 10
Rb+	PL	I-III	7.50(2.56), 10	20.25(5.14), 8	16.20(6.79), 10	9.65(2.43), 10
		V-VI	48.80(7.69), 10	70.69(8.14), 8	57.85(10.41), 10	41.40(5.52), 10
	IL	I-III	1.30(0.69), 10	3.13(1.32), 8	4.85(2.33), 10	2.55(1.55), 10
		V-VI	9.25 (3.90), 10	18.63(5.57), 8	15.60(4.87), 10	10.15(5.46), 10

FIGURE 8.

Immunization

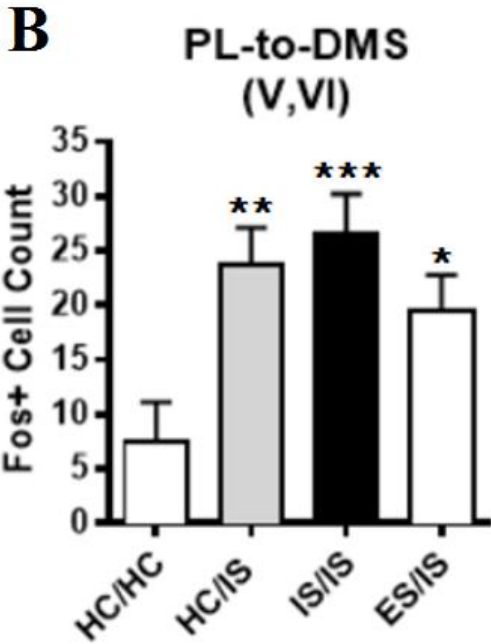
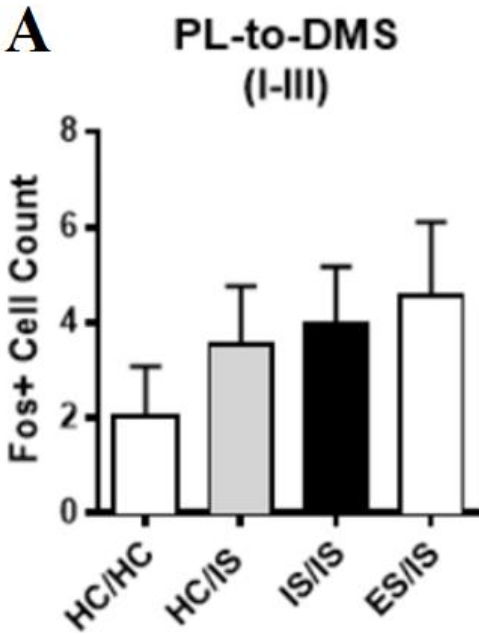


FIGURE 9.

Immunization

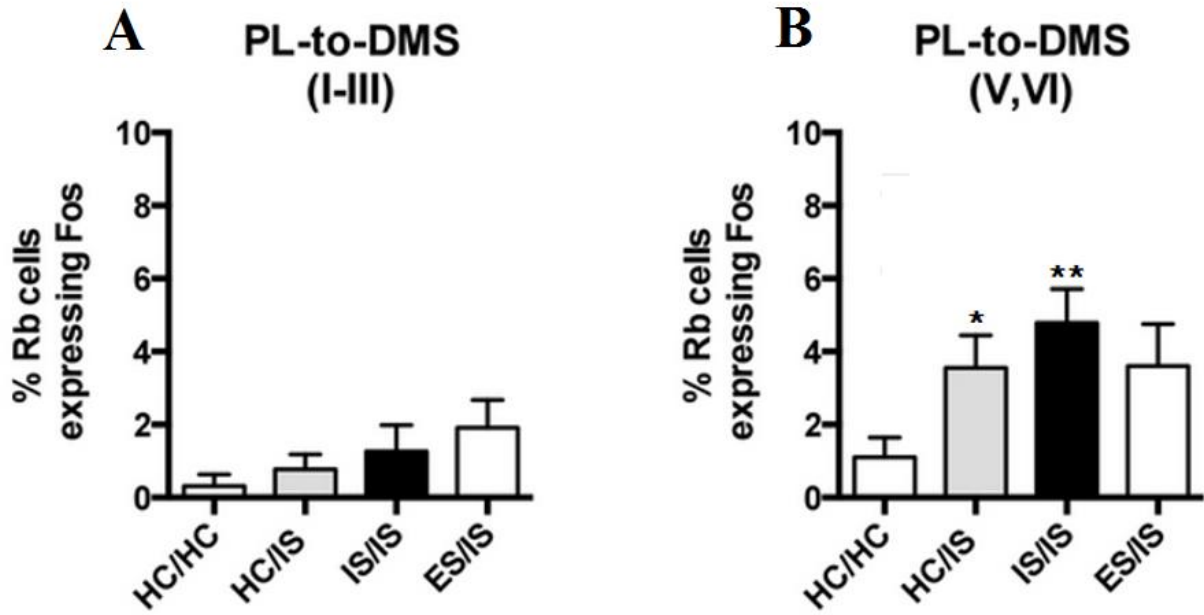


FIGURE 10.

